PARAMAGNETIC Fe³⁺: A SENSITIVE PROBE FOR DISORDER IN KAOLINITE

J.-M. Gaite,[1] P. Ermakoff,[1] Th. Allard[2] and J.-P. Muller[2,3]

[1] Centre de Recherche sur la Matière Divisée, Université d'Orléans-CNRS,
Rue de Chartres-BP 6759 - 45067 Orleans Cedex 2, France

[2] Laboratoire de Minéralogie-Cristallographie. Université de Paris VI et VII, 4, Place Jussieu - 75252 Paris Cedex 5, France

[3] ORSTOM, Département T.O.A. UR12, Géosciences de l'Environnement Tropical,
32 Avenue Henri Varagnat - 93143 Bondy Cedex, France

Abstract—The Fe^{3+} substituted for Al^{3+} at the 2 octahedral positions is one of the most common impurities in the kaolinite structure detected by electron paramagnetic resonance (EPR). Evidence has been provided for a relationship between the shape of EPR spectra for structural Fe and the structural disorder in kaolinite. It is proposed that the structural Fe be used as a sensitive probe for the degree of disorder of natural kaolinites. With this aim in view, an EPR disorder index (E) is defined from the width of selected EPR lines. Using reference kaolinites, it is shown that this index can account as well for long-range disorder detected by means of X-ray diffraction (XRD) as for local perturbations such as radiation-induced defects (RID). It is shown that the disorder observed through EPR has some points in common with the XRD-measured one. The influence on E of the presence of RID is shown by the study of artificially and naturally irradiated kaolinites.

Key Words—Disorder, Electron Paramagnetic Resonance (EPR), Fe^{3+}, Irradiation, Kaolinite, Point Defect.

INTRODUCTION

Many studies have described the structural perfection of kaolinites, reflecting the necessity of relating the properties that are exploited by industry. According to their conditions of genesis, natural specimens exhibit a wide variability of degrees of disorder that are clearly manifested in XRD patterns (Brindley and Brown 1980; Giese 1988).

Several attempts have been made to estimate this degree of disorder by proposing indices based on simplified determinations of peak and local background intensity ratios in selected parts of the diffractograms. These include the widely used Hinckley Index (HI) (Hinckley 1963), and the Liétard Index (R2) (Liétard 1977; Cases et al. 1982). Correlations were evidenced between such indices and spectroscopic information derived from sources such as the OH stretching band of Fourier transform infrared (FTIR) spectra or the relative distribution of structural Fe as assessed by EPR (Jones et al. 1974; Meads and Malden 1975; Mestdagh et al. 1980; Mestdagh et al. 1982; Cases et al. 1982; Brindley et al. 1986). The above-mentioned indices (HI and R2) lack sufficient information on the type and abundance of defects, but are still convenient for typology purposes. Such approaches remain empirical as long as no physical interpretation can be elucidated from a proper defect-structure model.

More detailed pictures of the nature and abundance of structural defects have been successively reported in the literature, involving various kinds of stacking faults to account for the XRD patterns (Giese 1988).

The most recent models were supported by matrix calculations using physically meaningful parameters and taking into account the real structure of the kaolinite layers. Successful descriptions of the XRD patterns were achieved by Plançon et al. (1988, 1989), Bookin et al. (1989) and Plançon and Zacharie (1990), by involving translations between B layers, minor presence of C layers and possible occurrence of 2 populations of kaolinites with contrasted defect structures. More recently, Artioli et al. (1995) proposed a model based on 4-layer stacking (B, C layers and their enantiomorphs) coupled to electrostatic energy calculations, which also satisfactorily reproduced the variability of kaolinite XRD patterns.

Besides the justified attention drawn to the large-scale disorder of natural kaolinites, which dominates XRD patterns, only a few works were conducted in order to give insight, even indirectly, into the defect structure at the local scale. For instance, the studies of kaolinites by ¹H NMR (Stone and Torres-Sanches 1988) and ²⁹Si, ²⁷Al magic angle spinning (MAS) NMR (Schroeder and Pruett 1996) found the existence of an heterogeneous distribution of paramagnetic impurities, consisting in diluted or clustered populations. In the present paper, we propose to use structural Fe itself as a probe for disorder involving long-range defects as well as point defects. Several justifications may support this proposal. Structural trivalent Fe is known to occur as a main impurity in all natural kaolinites (Mestdagh et al. 1980). On account of its sensitivity to the crystal field, information about the per-

fection of the crystal environment can be theoretically deduced from the EPR spectra of structural Fe^{3+}, as suggested by Gaite et al. (1993). The Fe^{3+} EPR spectra in kaolinite have been described as arising from 2 environments differing by their crystal field symmetry, and referred to as $Fe_{(I)}$ and $Fe_{(II)}$ (Jones et al. 1974; Mestdagh et al. 1980). The $Fe_{(I)}$ could correspond to disturbed environments at the limits of coherent domains (Noble 1971; Hall 1980), but no complete explanation has yet been published. On the other hand, it has been recently shown that the $Fe_{(II)}$ lines belong to 2 slightly different EPR spectra arising from Fe^{3+} substituted for Al^{3+}, at the 2 inequivalent octahedral positions in the kaolinite structure (Gaite et al. 1993), in total agreement with the structure refinement by Bish and Von Dreele (1989). As the line widths are sensitive to crystal imperfections, their measurement can be used as an index to describe the degree of disorder of kaolinite.

The aim of this study is to point out the sensitivity of the structural Fe^{3+} probe to the long-range defect structure of kaolinites, as appreciated through XRD, and to short-range disorder due to point defects, such as that produced by artificial or natural irradiations.

MATERIALS AND METHODS

Samples

Eleven reference samples were selected from numerous kaolinites originating from hydrothermal alteration, sediments and soils, in order to cover as continuously as possible the widest range of degrees of disorder. Most of these samples have been previously investigated in the literature. They are listed in Table 1 together with their sources, references, mineralogy and the various indices or parameters used in this study.

In order to include disorder induced by natural irradiation, several kaolinites originating from the uranium-rich hydrothermally altered volcanic tuffs at Nopal site, Chihuahua, Mexico (Muller et al. 1990; Leslie et al. 1993) were also studied. They were selected according to their RID content as determined from the procedure of Clozel et al. (1994).

Methods

EPR spectra were recorded at X-band (9,3 Ghz) with various spectrometers. The 2 spectrometers most often used were a Varian 4502 and a Brucker ER200D. These 2 spectrometers were equipped with a variable temperature unit using liquid nitrogen cooling temperatures as low as 90 K. They were modified in order to obtain numeric records of spectra. For both, the modulation frequency was 100 kHz. The magnetic field and the resonant frequency were calibrated accurately.

The XRD data were obtained with a PW 1710 vertical goniometer using monochromatic $CoK\alpha$ radiation

(40 kV, 30 mA) at scanning rates of 1 °2θ/90 s, for rapid acquisition of diffractograms, and a horizontal goniometer using monochromatic $CuK\alpha$ radiation (40 kV, 20 mA) with a 10 °2θ linear detector (INEL) for precise profile acquisition. Random powder mounts were prepared according to the back-loaded method (Moore and Reynolds 1989).

Several samples were irradiated with He^+ ions and γ-rays in order to simulate the effects of 2 main ionizing radiations occurring in natural systems, α-particles and γ-rays. Irradiation produces 3 types of electron-hole defects associated with oxygen atoms, referred to as B- ($Al-O^--Al$), A- ($Si-O^-$) and A'- ($Si-O^-$) centers, according to their nature and stability (Muller et al. 1992; Clozel et al. 1994, 1995).

1) The He^+ beam irradiations were performed on the ARAMIS ion accelerator (Orsay, France) with incident energies of 1.5 to 1.8 MeV. The characteristics of the accelerator used have been described in detail by Bernas et al. (1992). The experimental dose range of 5 kGy to 750 MGy was consistent with those encountered in natural systems (Allard et al. 1994). Samples were coated on metal plates by sedimentation in aqueous medium, resulting in an effective thickness of 2–3 μm. Dose was monitored with a systematic error of about ±10%.

2) The γ irradiations were carried out using a high dose-rate ^{60}Co source (16.7 ± 5% kGy/h) from the Centre d'Etudes Nucléaires de Grenoble (CENG, France). Samples were put in sealed glass containers and placed into a pool in the vicinity of the radiation source. Doses ranged from 0.03 to 30 MGy. This allowed comparison of γ radiation effects with those from α particles within a large dose range.

The irradiated samples were heated at 250 °C (2 h), and at 400 °C (24 h) in order to successively anneal the B- and A'-centers (Clozel et al. 1994).

THE PARAMAGNETIC IRON: A PROBE FOR CRYSTAL FIELD DISORDER

Origins of Line Broadening

Fe^{3+} in its fundamental configuration is in the state $^6S5/2$, which is very sensitive to the crystal field, which means to the environment of Fe^{3+} ion at short and even long range. A variation of the crystal field at Fe^{3+} vicinity produces a shift of the EPR transition lines, the importance of which depends on the considered line. As a consequence, if the environment of Fe^{3+} changes from one to another equivalent position in the structure, the average distribution of crystal fields will induce a broadening to the transition lines.

Several mechanisms may be responsible for line broadening:

1) The crystal field disorder. It can be classified schematically in 2 parts.

Table 1. Characteristics of the kaolinite samples studied.

Sample	Reference	Origin†	Aux. miner.‡	%Fe$_2$O$_3$	HI¶#	R2#	Exp. syst.††	$E_{RT}\cdot10^2$‡‡	$E_{140K}\cdot10^2$‡‡
DCV >2 μm	Gaite et al. 1993	Aveyron (1) (France)	—	0.25§	1.52	1.35	2 phases %wcp = 69	3.3	3.1
GB1	Cases et al. 1982	Cornwall (1) (GB)	M, Q	0.42 0.40§	1.29	1.13	2 phases %wcp = 54	7.4	6.2
GB3	Cases et al. 1982	Cornwall (1) (GB)	M, Q	0.57 0.53§	1.18	1.09	2 phases %wcp = 42	7.4	7.0
KGa-1	van Olphen and Fripiat 1979	Georgia (2) (USA)	A	0.24 0.21§	1.04	1.03	2 phases %wcp = 38	8.2	6.2
KGa-2	van Olphen and Fripiat 1979	Georgia (2) (USA)	A	1.16 0.88§	0.21	0.6	M = 91 Wc = 0.02 δ = 0.04 p = 0.35	11.3	10.0
BAR 1–2 μm	Clozel et al. 1994	Gironde (2) (France)	I	1.86§	0.37	0.86	M = 85 Wc = 0 δ = 0.04 p = 0.35	11.3	11.6
PDP3 <38 μm	Delineau et al. 1994	Charentes (2) France	G	0.27 0.23§	1.16	0.90	2 phases %wcp = 43	13.3	10.8
CHA2 <5 μm	Delineau et al. 1994	Charentes (2) (France)	I, Q	0.72 0.70§	0.25	0.52	M ≈ 66 Wc = 0.09 δ = 0.05 p = 0.40	14.4	12.2
FBT2 <38 μm	Delineau et al. 1994	Charentes (2) (France)	Q, A	1.05 0.83§	(0.28)	0.44	2 phases %wcp = 13	16.3	14.2
GOY <0.5 μm	Muller and Bocquier 1987	Goyoum (3) (Cameroon)	—	NM	(0.15)	0.49	M ≈ 68 Wc = 0 δ = 0.05 p = 0.35	16.4	15.6
U7	Cases et al. 1982	Charentes (2) (France)	Q, A	0.98 0.79§	0.29	0.23	M ≈ 49 Wc = 0.05 δ = 0.06 p = 0.40	17.0	14.0
Nopal samples									
C3	Muller et al. 1990	Chihuahua (1) (Mexico)	—	—	—	0.95	—	—	18.2
C15	Muller et al. 1990	Chihuahua (1) (Mexico)	—	—	—	1.30	—	—	3.9

† (1) Hydrothermal; (2) sediment; (3) soil.
‡ Auxilary minerals: Q, quartz; A, anatase; I, illite; M, mica; G, gibbsite.
§ Iron content measured on DCB deferrated samples.
¶ ( ) Nonreliable measurement due to noisy pattern.
# XRD indices: HI, Hinckley index; R2, Liétard index.
†† Exp. syst.: Expert system of Plançon and Zacharie (1990).
‡‡ EPR index: E measured at room temperature (RT) and 140 K.

The 1st kind of disorder is due to strains induced by the presence of defects at long range in the crystal. In layer silicates such as kaolinite, these defects may be related to stacking faults or to structural disorders inside the layers. Such defects lead to a modification of EPR spectra, and they are also detected by XRD.

In the structure, there may be some heterovalent ion substitutions, interstitial ions, vacancies or other electronic defects. The defects that influence the crystal field at the Fe^{3+} position (Gaite and Michoulier 1970), are not always detected by XRD.

2) The interaction between magnetic dipoles is referred to as "spin-spin interaction" (Abragam and Bleaney 1970). This cause of line broadening is important for the paramagnetic crystal, but is reduced in the case of diamagnetic hosts containing a low concentration of paramagnetic defects. Kaolinite is diamagnetic, but if charge defects, with a high concentration, are also paramagnetic, the spin-spin interaction can reinforce the line broadening.

The various origins of line broadening cannot easily be separated. In kaolinite they can all contribute to the observed line widths.

Definition of an EPR Disorder Index

X-band EPR spectra from selected samples of kaolinite are presented in Figure 1. EPR spectra show superimposed signals corresponding to trivalent Fe in 2 different sites with different distortion, referred to as $Fe_{(I)}$ and $Fe_{(II)}$ (Meads and Malden 1975). $Fe_{(I)}$ sites,
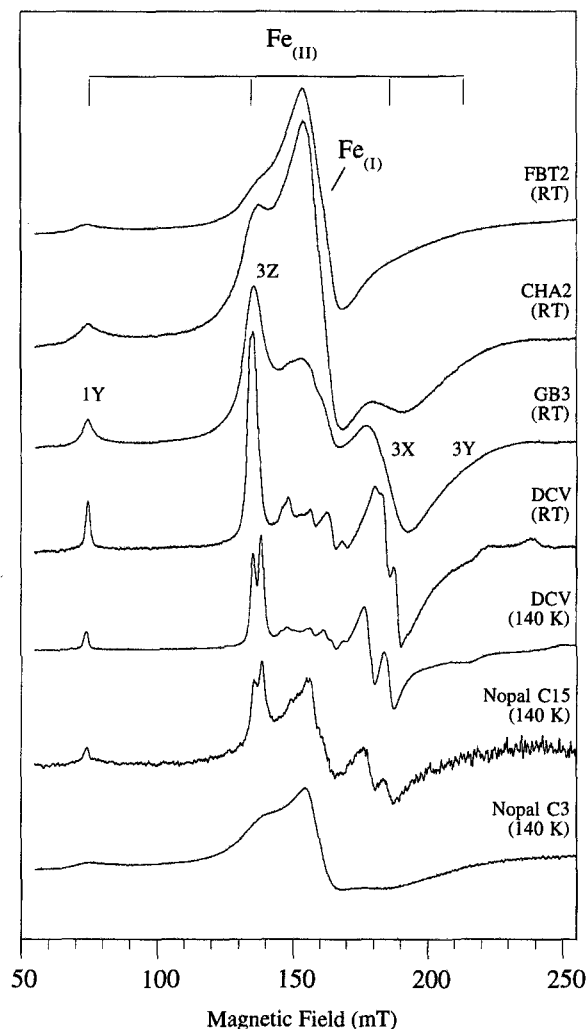
Figure 1. EPR spectra of different kaolinite samples, at X-band frequency (see Table 1 and "sample section" for identification). Fe^{3+} EPR transitions are labeled according to Gaite et al. (1993).

mT is often broad and partially masked by the $Fe_{(I)}$ spectrum (for example, sample CHA2). Only transitions 1Y at about 75 mT and 3Z at about 135 mT are always well observed. The 1Y line is isolated from any other transition, and its width can be measured in a simple manner. However, as it is the less-intensive line, its measurement may be inaccurate from noisy spectra. On the contrary, the 3Z line is intensive. However, at low temperature, it is not the exact superposition of the lines arising from the 2 octahedral irons, and the apparent width is increased. This effect is only observable for very well-crystallized samples (such as DCV and KGal), and can be disregarded at room temperature. Besides, this line is sometimes partially masked by the $Fe_{(I)}$ signal.

From previous considerations, it is proposed to define an EPR index based on the measurement of the width of the 1Y line, that is, independent of the frequency (within the X-band frequency domain) and of the magnetic scale of the EPR spectra.

Within the X-band frequency domain, the line width of the 1Y transition and the central magnetic fields for 3Z and 1Y lines are proportional to the frequency. Let us call D the distance of the lines 3Z and 1Y on the EPR spectra (Figure 2) and L the width of the 1Y line at half maximum. The ratio $E = L/D$ is dimensionless, independent of the frequency and on the scale of the EPR spectra. It only depends on the perfection of the crystal field around Fe^{3+}. Consequently, E can be used as a disorder index.

In few cases, the 1Y line may not intensive enough to be precisely measured (for example, sample FBT2). An alternative procedure for an EPR disorder index is to use the 3Z line width, leading to defining a parameter E_2. For those cases, only the low field region of the 3Z line is well-observable, hence, the line width is characterized by d, its half width at half maximum (Figure 2): $E_2 = d/D$. Although both lines 1Y and 3Z are unequally affected by crystal field imperfections (Gaite et al. 1993), it is verified that E and E_2 are linearly correlated: $E = 1.26 \times E_2 - 0.008$, with a correlation coefficient $r = 0.98$ at room temperature, as shown in Figure 3.

This relation is only suitable for EPR spectra recorded at room temperature. At low temperature, the resolution of signals being better, E is always measurable.

Properties of the EPR Index

The proposed EPR index is based upon the line width of a given EPR transition, and theoretically depends upon the occurrence of defects that may influence the crystal field. For this reason, it is not expected to be indicative of the nature and abundance of the relevant structural defects, either extended or point defects. Nevertheless, several main properties have to be emphasized:
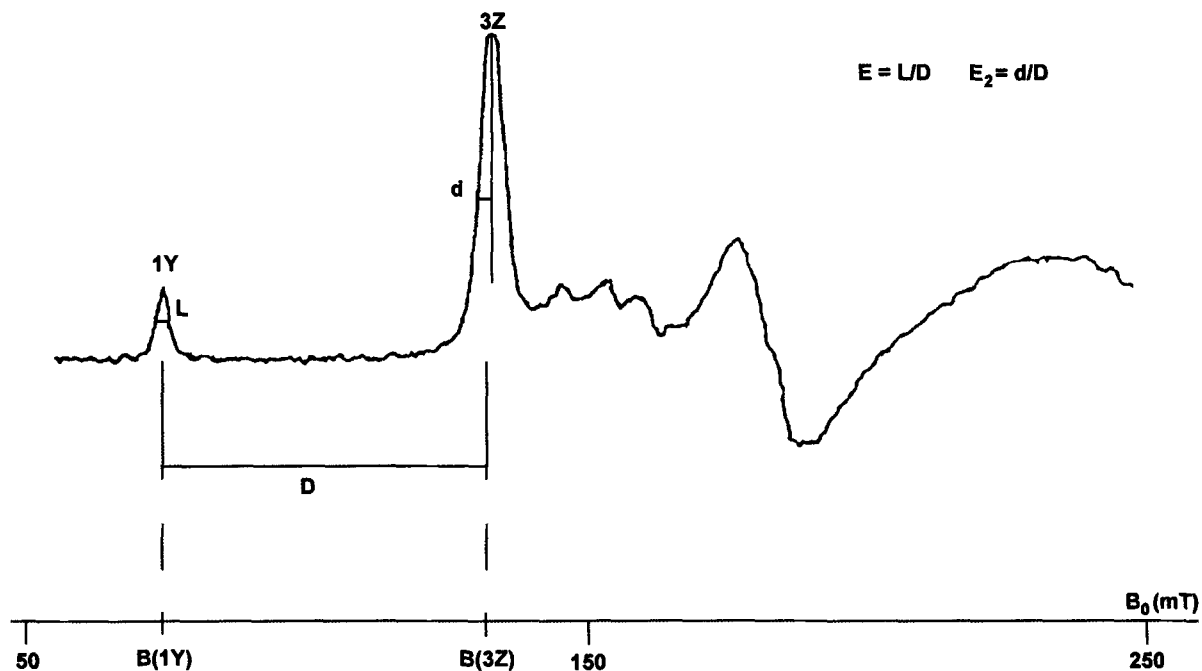
always present in relatively low concentration (Delineau et al. 1994), were suggested to be sites at the boundary of the XRD-coherent domains (Muller and Calas 1993). In contrast, $Fe_{(II)}$ sites have recently been demonstrated to correspond to Fe^{3+} substituted for the 2 nonequivalent Al^{3+} sites inside the kaolinite layer structure (Gaite et al. 1993), in agreement with the structure refinement by Bish and Von Dreele (1989).

The lines of the corresponding spectra, arising from the octahedral Fe^{3+} substituted for Al^{3+}, are labeled 1Y, 3X, 3Y, 3Z, according to Gaite et al. (1993). Since all lines are not equally sensitive to the crystal field imperfections, it is better to choose lines that could be used for an easy characterization of the sample.

The transition 3Y at about 200 mT is observed only for exceptionally well-crystallized kaolinite (such as sample DCV). Besides, the transition 3X at about 180

Figure 2. Fe^{3+} EPR spectrum of DCV kaolinite illustrating the determination of the indices E and E_2.

1) Orientation dependence. It is well known that kaolinite samples are often partially oriented. The relative intensities of the lines of the spectra depend on the degree of orientation but not the line shapes. Consequently, E is independent of a partial orientation of the particles within the sample.

2) Presence of auxiliary minerals. E is independent of the presence of other mineral phases within the sample. It was verified that the presence of the most common Fe-bearing accessory minerals (such as mica and gibbsite) in kaolin was not a limitation because of their undetectable or readily differentiated contributions to the signals in the low magnetic field region of the EPR spectra.

Figure 3.   Relation between E and E_2 indices at room temperature.

3) Temperature dependence. The EPR spectra are temperature-dependent (Figure 1). For comparative studies of different samples, it is thus necessary to determine E from spectra recorded at the same temperature. In any case, the temperature must be mentioned.

SENSITIVITY OF THE Fe PROBE TO VARIOUS KINDS OF DISORDER

Influence of Long-range Structural Defects

The width of the 1Y transition (E index) could be measured on the EPR spectra for all the kaolinite samples studied. An important and continuous variation of the E index was observed, with values ranging from $3 \cdot 10^{-2}$ to $17 \cdot 10^{-2}$, as reported in Table 1.

In order to test the sensitivity of the structural Fe probe to the long-range disorder, we 1st examined the information contained in XRD patterns presented in Figure 4.

As mentioned in the introduction, several approaches have been developed to describe the variability of degrees of disorder of natural kaolinites.

The expert system of Plançon and Zacharie (1990), based on the measurement of simple features of XRD patterns, was used. Four structural parameters were determined: the size of coherence domain (M) and the abundance of 3 kinds of structural defects (P: abundance of $+b/3$ translations; Wc: occurrence of C layers; δ: Gaussian distribution of translations). As can be seen in Table 1, a serious limitation of the expert system appears for more than half of our samples: the
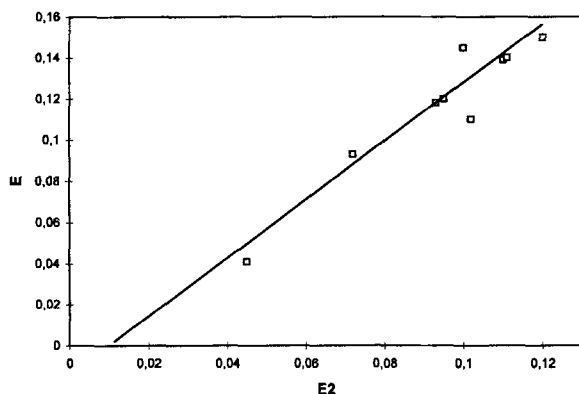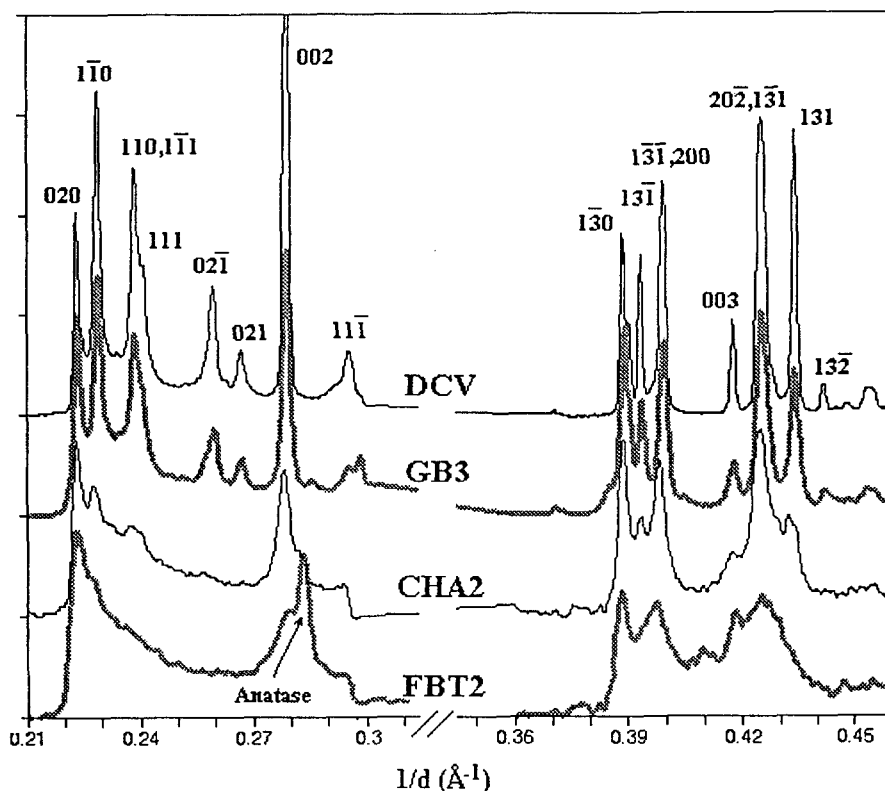
Figure 4. XRD patterns of selected kaolinite samples.

presence of 2 phases is determined together with the proportion of the well-crystallized phase (%wcp), but no information about their defect structure can be derived. That implies that the continuous variation of E cannot be related to the parameters derived from the expert system.

Although not fully informative, the measurement of the HI (Hinckley 1963) is an alternative way to differentiate the samples in terms of long-range structural perfection. HI is measured in the (021,111) XRD band where structural defects lead to the most noticeable variations. However, its use presents some limitations. On one hand, it cannot be reliably measured for several disordered samples (Table 1). On the other hand, Plançon et al. (1988, 1989) demonstrated that the HI is directly related to the abundance of defect-rich phase with respect to a low-defect phase. For a monophase kaolinite, Artioli et al. (1995) showed on simulated diffractograms that the HI decreases as the total density of defects increases. According to these considerations, the HI is reliable for at least 4 samples (KGa2, CHA2, BAR, U7).

Although somewhat unusual, the R2 index (Liétard et al. 1977; Cases et al. 1982) is useful to simply differentiate all the samples in terms of long-range structural perfection. The related R2 index, based on the variations in the (201,131) band (Figure 5), can be measured for the whole set of samples (Table 1). Its interpretation depends on the structural model used. According to Liétard, it depends on the presence of stacking faults and defects in the (a,b) plane, but this author does not give any physical explanation. According to Plançon et al. (1989, 1990) the (201,131) region is not affected by the $+b/3$ translations (with probability P), but is significantly affected by the Gaussian distribution of translations (δ parameter) and by the occurrence of C layers (Wc parameter). Finally, it can be verified that, according to Artioli et al. (1995) simulations, the R2 index decreases as the total density of defects increases. Thus, the R2 index can be considered as an appropriate way to differentiate the studied kaolinites in terms of long-range structural perfection. As shown in Table 1, the R2 index was the only one that could be measured for the whole set of samples.

The variation of R2 as a function of E is plotted in Figure 6. As can be seen, the EPR index increases as the XRD index decreases, whatever the fixed temperature of EPR spectra recording.

The dependence observed in Figure 6 shows that the structural Fe probe, sensitive to the variations of crystal field at Fe position, is related to the long-range disorder of the kaolinite. Consequently, the E index

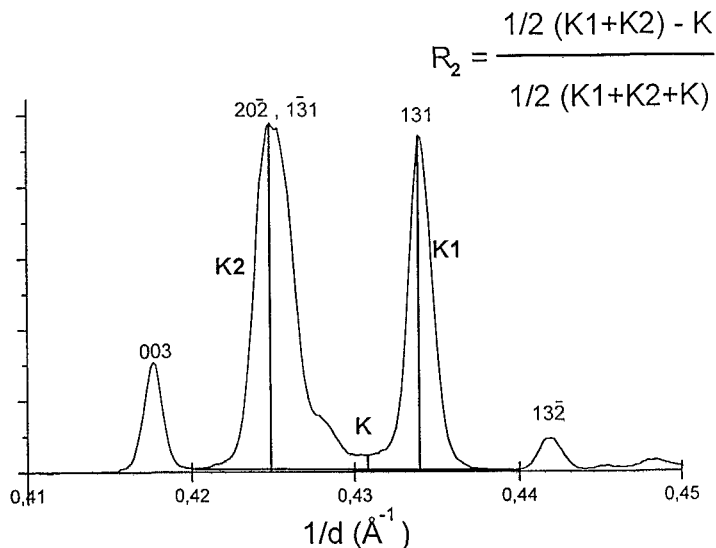$$R_2 = \frac{1/2\,(K1+K2) - K}{1/2\,(K1+K2+K)}$$

Figure 5. The (201,131) region of an XRD pattern illustrating the definition of the R2 (XRD) index.

can be used to estimate an average degree of disorder of natural kaolinite samples.

Similarly to R2, the HI index roughly decreases as E increases (Table 1). However, a substantial fluctuation is observed for the samples having an intermediate degree of disorder as appreciated with EPR (BAR, KGa2, PDP3).

Influence of Point-Defects: Artificially Irradiated Kaolinites

Figure 7 shows the low-temperature EPR of DCV kaolinite before and after α irradiation at 2 selected doses (2.3 and 230 MGy), together with a spectrum of irradiated DCV after heating at 400 °C. Increasing the radiation dose causes substantial and continuous changes to the EPR spectrum of Fe^{3+}. They are of 2 types:

1) An important increase of the intensity of a narrow transition in the region of $B = 150$ mT ($g = 4.3$). This behavior cannot be explained because the $Fe_{(I)}$ spectra are not yet fully elucidated.

2) A significant broadening of the $Fe_{(II)}$ lines without any shift in peak position.

On the contrary, the relevant XRD patterns did not exhibit any modification of relative peak intensities or widths. It can be inferred from these observations that
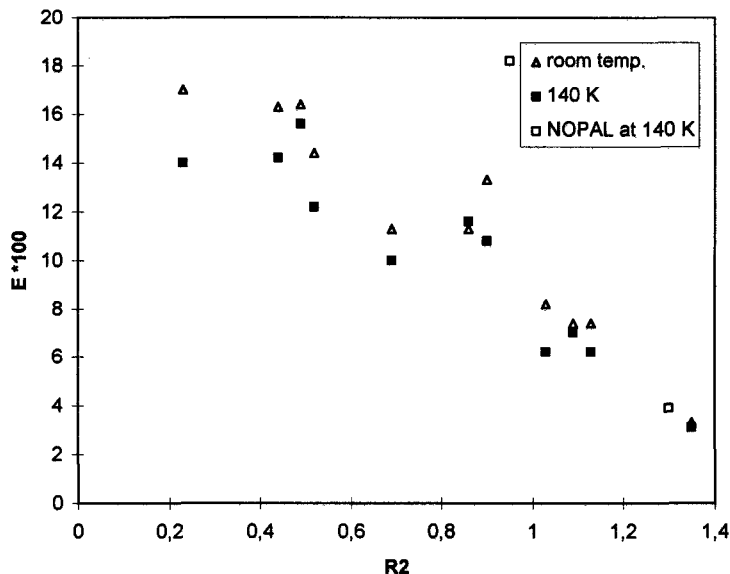

Figure 6. Relation between E (at room temperature and 140 K) and R2 indices for reference kaolinites.
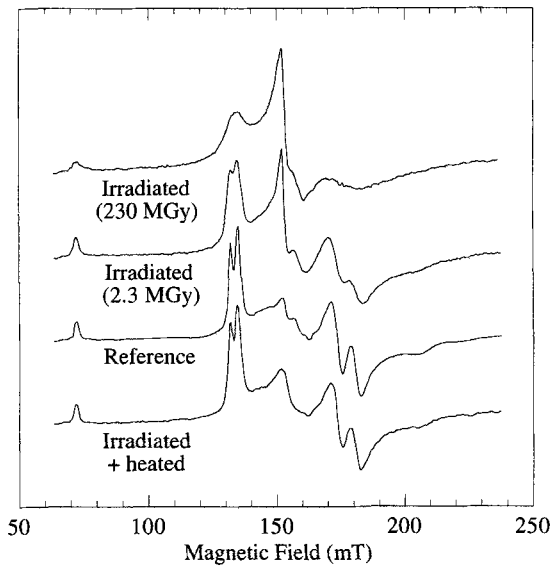
Figure 7. Modifications of Fe^{3+} EPR spectrum (at 93 K) of DCV after irradiation and subsequent heating.

Figure 9. Relation between the E index (at 93 K) for GBI and the concentration of B-centers produced by α and γ irradiations.

the applied irradiation induces a change of the crystal field at the Fe^{3+} positions, which is only due to a local disorder within the kaolinite structure. The $Fe_{(II)}$ lines of the spectrum of the irradiated DCV sample are narrowed after heating (400 °C during 24 h). Their shapes and their relative intensities become identical to the ones of the reference sample. This restoration of the local order means that the radiation-induced disorder in kaolinite structure, as revealed by the Fe^{3+} EPR probe, is reversible. Other heating experiments showed that the reversibility started at temperature as low as 250 °C (2-h heating). Similar results were obtained with GB1 and BAR samples, after γ irradiations.

These spectral modifications were quantified using the above-defined E disorder index. Figure 8 presents the variation of E (at 93 K) for GB1 sample (for which
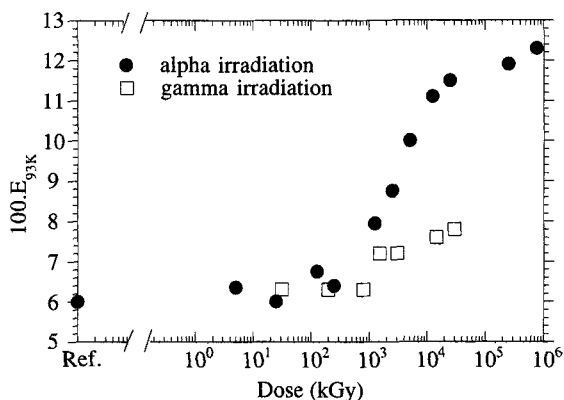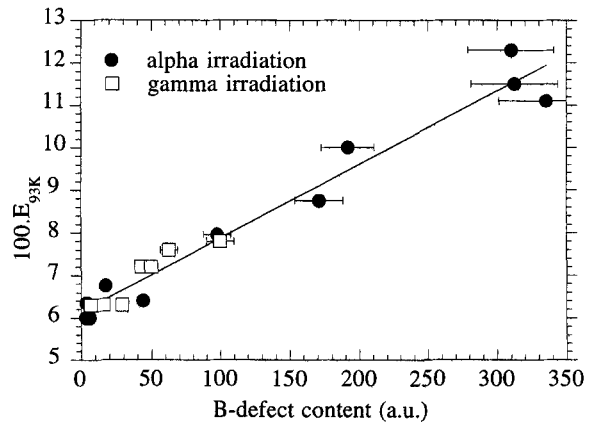
the most complete set of data was obtained), as a function of α and γ radiation doses. Two points must be noticed:

1) E remains quite constant ($E = 0.06$) up to a dose of 10^3 kGy and then markedly increases. An asymptote ($E = 0.12 - 0.13$) is reached for doses higher than 10^5 kGy,

2) The increase of E as a function of dose is stronger for the α-irradiated sample than for the γ-irradiated sample: for instance, at 20 MGy dose, the value for α irradiation is 50% higher.

In order to explain these results, it is necessary to specify the nature of the RIDs. Recent irradiation experiments with several natural kaolinites have shown that irradiations with He^+ beam and γ rays produce mainly B-centers, that is, $Al-O^--Al$ centers (Allard et al. 1994; Clozel et al. 1995). B-center concentration was at least 1 order of magnitude higher than the one of the other centers within the dose range investigated

Figure 8. Evolution of the E index (at 93 K) for GBI, as a function of α and γ radiation doses.
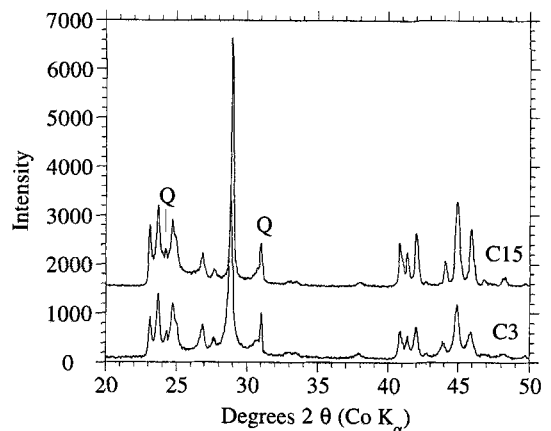

Figure 10. XRD patterns of Nopal kaolinite samples C15 and C3. Both samples contain a minor amount of quartz (Q).

Table 2. Some characteristics of various Nopal kaolinite samples.

Sample	$E_{(140K)} \cdot 10^2$	R2	[A'-center](a.u.)	[A-center](a.u.)
C15	3.9	1.30	6.3	10.0
B1	4.7	NM†	5.5	8.4
A2	4.7	NM	34.2	16.5
B2	5.4	1.32	11.0	8.3
B13	7.0	1.31	84.7	20.4
B4	10.1	1.27	74.0	14.6
C14	11.6	1.13	48.3	13.0
C3	18.2	0.95	115.0	16.1

† NM = nonmeasured.

Figure 11. Relation between E (at 140 K) and the concentration of A- and A'-centers in Nopal kaolinites.

(<750 MGy). Thus, it is of a special interest to consider the variation of E as a function of center concentration.

Figure 9 shows a strong relation between the E index and the B-center concentration, independently of the radiation used, which means that the crystal field at Fe^{3+} position is disturbed by the presence of these centers. The statistical density of radiation-induced B centers increasing with dose, the average distance between Fe and B-centers decreases. Because B-centers are paramagnetic, the broadening of EPR transition lines is due to the presence of point charge defects including dipolar interactions.

These results show that the structural Fe probe is sensitive to the presence of point defects, if their concentration is above a given limit (which could be estimated to 50 a.u., according to Clozel et al. 1994).

Influence of Point-defects: Naturally Irradiated Kaolinites

Figure 6 shows that the representative point of the sample Nopal C3 lies far from all others. This situation can be explained by the presence of point defects, at various concentrations, in the Nopal samples. Some characteristics of the Nopal samples are given in Table 2.

It was demonstrated that the concentration of RID in Nopal kaolinites varies substantially from the breccia pipe to the barren rock (Muller et al. 1990). The A'-centers appeared to be present in appreciable amounts when kaolinite was closely associated with U-bearing secondary minerals (Ildefonse et al. 1990, 1991).

The XRD patterns of the Nopal kaolinites are characteristic of well-ordered structures, as can be seen in Figure 10 for the 2 representative samples C3 and C15. Besides, these 2 kaolinites present contrasted Fe^{3+} EPR spectra (Figure 1). The spectrum of C15 is close to that of DCV, that is, the best-ordered reference kaolinite, whereas the spectrum of C3 is similar to that of FBT2, that is, the most badly ordered kaolinite. The values of E vary between 0.04 and 0.18, that is, they cover the whole range of disorder of the previously studied kaolinites. On the contrary, R2 values, al-
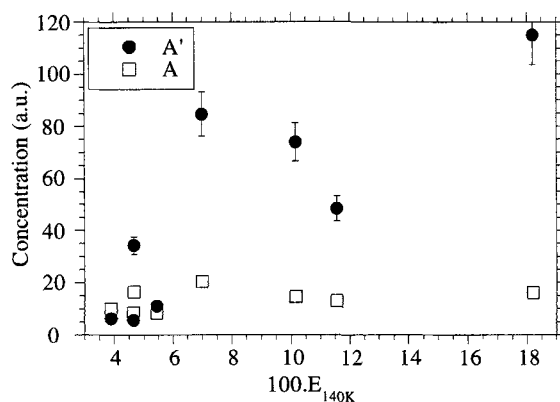
though different from one sample to the other, remain in a very limited range, from 0.9 to 1.3.

The influence of RID concentration on E index has been studied. The concentration of B-centers is very low; the only variation of E as a function of the concentration of A- and A'-centers is presented on Figure 11. This figure clearly shows that a correlation exits between E and A'-center concentration. This result strongly suggests that the local disorder affecting the Nopal kaolinites is essentially due to radiation damage.

The A'-centers are thought to result from the decoration of structural point defects as vacancies or interstitials, since they are expected to be produced dominantly by alpha recoil nuclei (Muller et al. 1992). Moreover, the A'-center annealing of several Nopal kaolinites (400 °C, 2 h) was not efficient enough to restore the EPR spectra of Fe^{3+}. The local disorder of the Nopal kaolinites is due to the presence of the paramagnetic centers A', but also to the consecutive occurrence of atomic displacements in the kaolinite structure produced by recoil nuclei.

CONCLUSION

Trivalent Fe in kaolinite can be used as a probe for structural disorder in kaolinite, since the line widths of Fe^{3+} EPR spectra are related to crystal field perturbations. An EPR index of disorder (E), very simple to use, dimensionless, independent of the microwave frequency and not sensitive to preferential orientations of the particles, can be defined. The study of a set of natural kaolinites, from very well to very badly crystallized, completed by the study of irradiated kaolinites, clearly shows that E allows assessment of long-range disorders, such as stacking faults, and local ones, related to point defects. The contribution to the E index of point charge defects can be partially reduced by heating kaolinite samples.

REFERENCES

Abragam A, Bleaney B. 1970. Electron paramagnetic resonance of transition ions. Oxford: Clarendon Pr. 911 p.

Allard T, Muller J-P, Dran J-C, Menager M-T. 1994. Radiation-induced paramagnetic defects in natural kaolinites: Alpha dosimetry with ion beam irradiation. Phys Chem Mineral 21:85–96.

Artioli G, Bellotto M, Gualtieri A, Pavese A. 1995. Nature of structural disorder in natural kaolinites: A new model based on computer simulation of powder diffraction data and electrostatic energy calculation. Clays Clay Miner 43:438–445.

Bernas H, Chaumont J, Cottereau E, Meunier R, Traverse A, Clerc C, Kaitasov O, Lalu F, Le Du D, Moroy G, Salomé M. 1992. Progress report on Aramis, the 2MV tandem at Orsay. Nucl Instrum Methods Phys Res B62:416–420.

Bish DL, Von Dreele RB. 1989. Rietveld refinement of nonhydrogen atomic positions in kaolinite. Clays Clay Miner 37:289–296.

Bookin AS, Drits VA, Plançon A, Tchoubar C. 1989. Stacking faults in the kaolin-group minerals in the light of real structural features. Clays Clay Miner 37:297–307.

Brindley, GW, Brown G. 1980. Crystal structures of clay minerals and their X-ray identification. London: Mineral Soc. p 495.

Brindley GW, Kao CC, Harrison J, Lipsicas M, Raythatha R. 1986. Relation between structural disorder and other characteristics of kaolinites and dickites. Clays Clay Miner 34:239–249.

Cases J-M, Liétard O, Yvon J, Delon J-F. 1982. Etude des propriétés cristallochimiques, morphologiques, superficielles de kaolinites désordonnées. Bull Mineral 105:439–455.

Clozel B, Allard T, Muller J-P. 1994. Nature and stability of radiation-induced defects in natural kaolinites: New results and reappraisal of published works. Clays Clay Miner 42:657–666.

Clozel B, Gaite J-M, J-P, Muller. 1995. Al-O⁻-Al paramagnetic defects in kaolinite. Phys Chem Mineral 22:351–356.

Delineau T, Allard T, Muller J-P, Barres O, Yvon J, Cases J-M. 1994. FTIR reflectance vs. EPR studies of structural iron in kaolinites. Clays Clay Miner 42:308–320.

Gaite J-M, Ermakoff P, Muller J-P. 1993. Characterization and origin of two Fe³⁺ EPR spectra in kaolinite. Phys Chem Mineral 20:242–247.

Gaite J-M, Michoulier J. 1970. Application de la résonance paramagnétique électrique de l'ion Fe³⁺ à l'étude de la structure des feldspaths. Bull Soc Fr Mineral 93:341–356.

Giese RF Jr. 1988. Kaolin minerals: Structures and stabilities. In: Bailey SW, editor. Kaolin minerals: Structures and stabilities. Washington, DC: Mineral Soc Am. p 29–66.

Hall PL. 1980. The application of spin resonance spectroscopy to studies of clay minerals. Clay Miner 15:321–351.

Hinckley DN. 1963. Variability in "crystallinity" values among the kaolin deposits of the coastal plain of Georgia and South Carolina. Clays Clay Miner 13:229–235.

Ildefonse P, Muller JP, Clozel B, Calas G. 1990. Study of two alteration systems as natural analogues for radionuclide release and migration. Eng Geol 29:413–439.

Ildefonse P., Muller J-P, Clozel B, Calas G. 1991. Record of past contact between altered rocks and radioactive solutions through radiation-induced defects in kaolinite. Mater Res Soc Symp Proc:749–756.

Jones JP, Angel BR, Hall PL. 1974. Electron spin resonance studies of doped synthetic kaolinites. Clay Miner 10:257–259.

Leslie BW, Pearcy EC, Prikryl JD. 1993. Oxidative alteration of uraninite at the Nopal I deposit, Mexico: Possible contaminant transport and source term constraints for the proposed repository at Yucca Mountain. MRS Symp Proc 294:505–512.

Liétard O. 1977. Contribution à l'étude des propriétés physicochimiques cristallographiques et morphologiques des kaolins [Doctoral d'Etat]. Spécialité Sciences Physiques. Lorraine, France: Institut National Polytechnique de Lorraine.

Meads RE, Malden PJ. 1975. Electron spin resonance in natural kaolinites containing Fe³⁺ and other transition metal ions. Clay Miner 10:313–345.

Mestdagh MM, Herbillon AJ, Rodrique L, Rouxhet PJ. 1982. Evaluation du rôle du fer structural sur la cristallinité des kaolinites. Bull Mineral 105:457–466.

Mestdagh MM, Vielvoye L, Herbillon AJ. 1980. Iron in kaolinite: II. The relationship between kaolinite crystallinity and iron content. Clay Miner 15:1–13.

Moore DM, Reynolds RC Jr. 1989. X-ray diffraction and the identification and analysis of clay minerals. New York: Oxford Univ Pr. 332 p.

Muller J-P, Bocquier G. 1987. Textural and mineralogical relationships between ferruginous nodules and surrounding clay matrices in a laterite from Cameroon. In: Schultz LG, van Olphen H, Mumpton FA. Proc Int Clay Conf; 1985; Denver, CO. Bloomington, IN: Clay Miner Soc. p 186–194.

Muller J-P, Calas G. 1993. Genetic significance of paramagnetic centers in kaolinites. Boulder, CO: Clay Miner Soc. p 261–289.

Muller J-P, Clozel B, Ildefonse P, Calas G. 1992. Radiation-induced defects in kaolinite: Indirect assessment of radionuclide migration in the geosphere. Appl Geochem 1:205–216.

Muller JP, Ildefonse P, Calas G. 1990. Paramagnetic defect centers in hydrothermal kaolinite from an altered tuff in the Nopal Uranium deposit, Chihuahua. Mexico. Clays Clay Miner 38:600–608.

Noble FR. 1971. A study of disorder in kaolinite. Clay Miner 9:71–81.

Plançon A, Giese RF, Snyder R. 1988. The Hinckley index for kaolinites. Clay Miner 23:249–260.

Plançon A, Giese Jr RF, Snyder R, Drits VA, Bookin AS. 1989. Stacking faults in the kaolin-group minerals: Defect structures of kaolinite. Clays Clay Miner 37:203–210.

Plançon A, Zacharie C. 1990. An expert system for the structural characterization of kaolinites. Clay Miner 25:249–260.

Schroeder PA, Pruett RJ. 1996. Fe ordering in kaolinite: Insights from ²⁹Si and ²⁷Al MAS NMR spectroscopy. Am Mineral 81:26–38.

Stone WEE, Torres-Sanchez RM. 1988. Nuclear magnetic resonance spectroscopy applied to minerals. Structural iron in kaolinites as viewed by proton magnetic resonance. J Chem Soc, Faraday Trans 1-84:117–132.

van Olphen H, Fripiat JJ. 1979. Data Handbook for clay minerals and other non-metallic minerals. Pergamon Pr 346 p.